Hierarchical Energy Management System for Home Microgrids

Fengji Luo, *Member*, *IEEE*, Gianluca Ranzi, *Member*, *IEEE*, Shu Wang, and Zhao Yang Dong, *Fellow*, *IEEE*

***Abstract*—With the spread of distributed energy resources, sensing infrastructure, and automation facilities, modern homes are becoming "home microgrids". This paper intends to support this trend and proposes a two-stage hierarchical energy management system for smart homes by considering both day-ahead and actual operation stages. In the day-ahead stage, an efficient scenario analysis approach is developed to account for the residential photovoltaic solar power uncertainty. The approach performs solar power scenario generation and reduction based on the Wasserstein distance metric and K-medoids, respectively. This is then followed by the use of a stochastic day-ahead residential energy resource scheduling model. In the actual operation stage, a Semi-Scenario based Rolling Horizon Optimization (SSRHO) mechanism is proposed, based on which an actual operation model is established. Simulations are then conducted to validate the effectiveness of the proposed system.**

[1]***Index Terms*—Nanogrid, smart home, demand response, demand side management, building automation**

NOMENCLATURE

Indices and Sets

o, O	Index and set of the solar power scenario;
a, Φ	Index and set of the controllable appliances;
a', Φ^{ICA}	Index and set of the interruptible controllable appliances;
a'', Φ^{NICA}	Index and set of the non-interruptible controllable appliances;

Constants

ρ_o	Occurrence probability of the solar power scenario o;
T	Total number of scheduling time intervals;
T^{pd}, T^{sn}	Total number of time intervals of the prediction window and scenario window;
Δt	Duration of scheduling time interval (hour);
d_a	Duration of a full operation cycle of the controllable appliance a (hour);
P_a^{ca}	Rated power of the ith controllable appliances (kW);
$P_a^{ca,base}$	Base power of the ith controllable appliances (kW);
δ_i^{begin} , δ_i^{end}	User preferred operation time range of ith controllable appliance;
L_t	Must-run home load at time t (kW, excluding the controllable appliances);
L_t^{srho}	Total home load at time t of the SSRHO stage (kW, including the controllable appliances);
pr_t	Electricity price at time t ($/kWh);
$E^{bess,rate}$	Energy capacity of the RBESS (kWh);
$P_{o,t}^{pv}$	Solar power output at time t under scenario o (kW);
$P_t^{pv,pd}$	Predicted PV solar power (kW) at time t of the prediction window;
$P_{o,t}^{pv,sn}$	Predicted PV solar power (kW) at time t of the scenario window under scenario o;
t_a^{begin}, t_a^{end}	Begin and end time of the user's preferred operation time ranges of controllable appliance a;
$P^{bess,rate}$	Rated power of the RBESS (kW);
γ	Cost coefficient of the RBESS;
$SOC^{\min}$	Lower SOC limit of the RBESS;
$SOC^{\max}$	Upper SOC limit of the RBESS;
η^c, η^l	Charging loss (%) and leakage loss factors (%/month) of the RBESS;
SOC^{desire}	Minimum SOC level of the RBESS desired by the user at the end of the scheduling horizon;
$\tau_{\min,i}^{on}, \tau_{\min,i}^{off}$	Minimum online and offline limits of ith ISA at t (hour);

Variables

$s_{a,t}$	Status of the controllable appliance a at time t under solar power scenario o: 1-ON, 0-OFF;
$L_{o,t}^{net}$	Net-power consumption of the house at time t under solar power scenario o (kW);
P_t^{bess} , $P_t^{bess,srho}$	Charging/discharging power of the RBESS at time t (kW) of the day-ahead stage and SSRHO stage respectively: positive-charging, negative-discharging;
E_t^{bess} , $E_t^{bess,srho}$	Remaining energy in the RBESS at time t (kWh) of the day-ahead stage and SSRHO stage, respectively;
$\tau_{a,t}^{on}, \tau_{a,t}^{off}$	Accumulated online and offline durations of controllable appliance a at time t (hour);
SOC_t	SOC of the RBESS at time t;

This work is supported by the Australian Research Council through its Future Fellowship scheme (FT140100130), in part by an Australian Research Council Discovery Projects (DP170103427) (DP180103217).

[1] F. Luo and G. Ranzi are with the School of Civil Engineering, University of Sydney, NSW, Australia (Emails: fengji.luo@sydney.edu.au; gianluca.ranzi@sydney.edu.au);

S. Wang and Z.Y. Dong are with the School of Electrical and Information Engineering, University of New South Wales, NSW, Australia (Emails: shu.wang1@student.unsw.edu.au; joe.dong@unsw.edu.au)

I. Introduction

RECENT TECHNICAL ADVANCES of two-way communication, Advanced Metering Infrastructure (AMI), distributed energy resources, and building automation facilities have contributed to the development of smart home applications. Modern homes are currently evolving towards small cyber-physical systems that are capable to simultaneously generate and consume energy. These systems have been usually referred to as "nanogrids" or "home microgrids" [1].

The Home Energy Management System (HEMS) plays a critical role in the energy optimization of a smart home because it acts like an expert system that serves the residential user in a residential unit/house. HEMSs usually coordinate home energy resources (HERs) and provide decision-making support for residential users. In the literature, HEMS has been extensively studied. In [2], Zhao *et al*. propose a HEMS model to optimally schedule the operation of household appliances under a real-time electricity pricing. Pedrasa *et al*. [3] optimally schedules a Residential Battery Energy Storage System (RBESS) and household appliances with rooftop solar power penetration. In [4], a load commitment framework is proposed to minimize the household operation cost. In [5], a HEMS is designed to dynamically schedule appliances in each dwelling unit based on which the power demand of the whole community is forecasted and reported to the utility. The work presented in [6] proposes a two-stage HEMS where, in the first stage, the charging/discharging of a RBESS is optimally scheduled based on the forecasted solar power and, in the second stage, the actual charging/discharging of the RBESS is determined based on actual solar power output. The work in [6] is based on a rule-based RBESS charging/discharging update mechanism that would not necessarily produce optimal solution over a finite horizon and it doesn't consider the demand response flexibility of household appliances. [7] studied coordinated scheduling of Heating, Ventilating, and Air Conditioning (HVAC) system and home plugged EV. [8] proposes an appliance scheduling model subjected to a combined tariff structure of real-time pricing and inclining block rates. [9] proposes an optimization scheme for residential solar water heaters, with the aim to minimize the peak-power consumption of a residential unit. In our recent work, we study the development of HEMS with Vehicle-to-Home (V2H) technology and residential photovoltaic solar power [10]. In [11-13], we propose a version of residential energy management system, i.e. "demand side recommender system" that uses personalized recommendation technology to recommend energy-aware products/suggestions to residential users and does not automatically control the home energy resources. Therefore, the work in [11-13] aims to improve awareness of users on demand response, and is essentially different with home automation systems such as the one that is presented in this paper.

With increasing penetration of renewables, the stochastic nature of renewable energy becomes a non-neglectable factor in home energy management. Despite the large number of available research, only few papers have considered the uncertainty in the home environment. [14] develops a HEMS to consider the worst case of forecasted solar power output, even if this strategy would lead to over pessimistic solutions. [15] proposes a home energy management strategy to take into account the uncertainty of real-time pricing (RTP). [16] develops a stochastic HEMS, which uses Monte-Carlo sampling technique to sample trip rate of the unit. Recent research [17-20] uses Model Predictive Control (MPC) technique to control thermostatically controlled household appliances when exposed to uncertain renewable energy output. In particular, [17] and [18] compare MPC controller with ON/OFF controller and PID controller on air conditioning systems; [19] and [20] use MPC to control three thermostatically controlled appliances: air conditioner, water heater, and refrigerator, with the objective to reduce the peak-hour household energy demand.

This paper proposes a hierarchical energy management system for smart homes with high photovoltaic (PV) solar power penetration. The proposed system considers the stochastic nature of the residential solar power in both day-ahead scheduling and actual operation stages. Main contributions of this paper are presented as follows:

(1) In the day-ahead stage, a residential solar power scenario analysis approach is developed based on the Wasserstein distance metric and K-medoids. The developed approach is computational efficient and suitable for residential energy management systems that are generally deployed on devices with limited computing power, such as smart meter, smart phone, and personal computer;

(2) based on the solar power scenario analysis, a stochastic day-ahead HER scheduling model is proposed to minimize the expected home electricity cost over the scheduling horizon;

(3) A new variation of the rolling horizon optimization (RHO) technique is proposed and referred to as the Semi-Scenario based Rolling Horizon Optimization (SSRHO). Different from conventional RHO that only consists of a point prediction window, SSRHO sets up a point prediction window and a stochastic window, and integrates the scenario analysis within RHO. The proposed SSRHO interacts with the home operation model that updates charging/discharging of the residential battery energy storage system (RBESS) based on the day-ahead scheduling result.

Compared with many existing works that only consider day-ahead scheduling of home energy resources (e.g. [2-4], [8-10]), the novelty of the proposed HEMS relies in combining the following points: system coordination of both day-ahead scheduling and actual operation stages to sufficiently consider the influence of renewable output uncertainty; the use of a RBESS control in both day-ahead and actual operation stages; the system links the penetration of multiple controllable household appliances with scenario analytics method to account for the renewable energy's probabilistic nature; computationally efficient, when compared to other conventional scenario analytics techniques, such as the Monte-Carlo method (as demonstrated in the simulation results' section of the paper); , integration of the scenario analytics into conventional RHO/MPC (where 'MPC' and 'RHO', used in automatic control and optimization domains, respectively, depict the same type of process as discussed in Section III), therefore enabling the applicability of the approach to longer control window where point prediction is not applicable.

This rest of this paper is organized as follows: Section II presents the scenario analysis methodology of PV solar power; Section III introduces the proposed hierarchical HEMS; Section IV presents the solving approach; Section V discusses the

simulation results; conclusions are drawn in Section VI.

II. Scenario Analysis of Residential PV Solar Power

High intermittence and volatility of solar power represent a significant management challenge for effective home energy management solutions. In this study, a new scenario analysis approach that integrates Wasserstein distance-based scenario generation and K-medoids based scenario reduction is developed to effectively tackle the solar power uncertainty. The Wasserstein metric distance and K-medoids have already been used in energy applications [21, 23] as useful scenario analytics techniques while, to the knowledge of the authors, this is the first use of this technique for home energy management.

A. Wasserstein Based PV Solar Power Scenario Generation

The PV solar power output is expressed as [22]:

$$P_p = E \cdot A \cdot \tau \tag{1}$$

where E represents the light intensity; A denotes the solar field size; τ is the photoelectric conversion rate.

The probability density function of light intensity $P_c(E)$ can be modelled as the two-parameter beta distribution [23]:

$$f(E) = \frac{\Gamma(\alpha+\beta)}{\Gamma(\alpha)\Gamma(\beta)}\left(\frac{E}{E_{\max}}\right)^{\alpha-1}\left(1-\frac{E}{E_{\max}}\right)^{\beta-1} \tag{2}$$

where E_{max} is the maximum light intensity; α and β are shape parameters, which can be obtained through curve fitting.

Based on models (1) and (2), the probability density function of the PV solar power can be obtained as follows:

$$f(P_P) = \frac{\Gamma(\alpha+\beta)}{\Gamma(\alpha)\Gamma(\beta)}\left(\frac{P_P}{P_{P\max}}\right)^{\alpha-1}\left(1-\frac{P}{P_{\max}}\right)^{\beta-1} \tag{3}$$

where P_{Pmax} is the maximum output of the PV power. For each hour, the number of discrete quantiles Q is determined based on the value of P_{Pmax}.

The Wasserstein distance metric, which has been proven to outperform many other methods [24], is applied to discretize the continuous distribution of PV solar power. In Wasserstein distance metric, a distance measurement between two probability distributions, denoted as W_r, is defined as:

$$W_r(p_1, p_2; \pi) = \int \pi\left[p_1(x), p_2(x)\right]^r dx \tag{4}$$

where p_1 and p_2 are two probability density functions; π (p_1, p_2) is the distance measurement; and r denotes the order.

Finding the most similar discrete probability function of a known continuous probability distribution is equivalent to calculating the minimum W_r. By assuming that the continuous probability function of variable x is $P_c(x)$, its optimal discrete quantiles z_q (q=1, 2…, Q) can be calculated as:

$$\int_{-\infty}^{z_q} P_c(x)^{1/(1+r)} dx = \frac{2q-1}{2Q}\int_{-\infty}^{\infty} P_c(x)^{1/(1+r)} dx \tag{5}$$

By substituting density function (3) into the Wasserstein scenario generation of Eq. (5), the discrete probability function of solar power can be expressed as:

$$\begin{aligned}&\int_{-\infty}^{z_q}\left(\frac{P_p}{P_{p\max}}\right)^{\frac{\alpha-1}{1+r}}\left(1-\frac{P_p}{P_{p\max}}\right)^{\frac{\beta-1}{1+r}} d\left(\frac{P_p}{P_{p\max}}\right) = \\ &\frac{2q-1}{2Q}\int_{-\infty}^{\infty}\left(\frac{P_p}{P_{p\max}}\right)^{\frac{\alpha-1}{1+r}}\left(1-\frac{P_p}{P_{p\max}}\right)^{\frac{\beta-1}{1+r}} d\frac{P_p}{P_{p\max}}\end{aligned} \tag{6}$$

Let $t = \frac{P_p}{P_{p\max}} \in (0,1)$, $\mu = \frac{\alpha+r}{1+r} > 0$, $\theta = \frac{\beta+r}{1+r} > 0$, Eq. (6) can be rewritten as:

$$\int_0^{z_q} t^{\mu-1}(1-t)^{\theta-1} dt = \frac{2q-1}{2Q}\int_0^1 t^{\mu-1}(1-t)^{\theta-1} dt \tag{7}$$

The right side of Eq. (6) satisfies the form of the B function, i.e. $\frac{2q-1}{2Q}.\frac{\Gamma(\mu)\Gamma(\theta)}{\Gamma(\mu+\theta)}$, while the left side of the same equation satisfies the incomplete B function, i.e. $B(z_q;\mu,\theta).\frac{\Gamma(\mu)\Gamma(\theta)}{\Gamma(\mu+\theta)}$. Based on these considerations, Eq. (7) can be rearranged as:

$$B(z_q;\mu,\theta) = \frac{2q-1}{2Q} \tag{8}$$

The probability of each optimal discrete quantile P^q, can be obtained as specified in Eq. (9), where $P_p(x)$ denotes the probability density function of solar power.

$$\begin{cases} P^q = \int_{\frac{z_{q-1}+z_q}{2}}^{\frac{z_q+z_{q+1}}{2}} P_p(x)dx, q = 1,...,Q \\ P^0 = \int_{z_0}^{\frac{z_1+z_2}{2}} P_p(x)dx \\ P^{Q+1} = \int_{\frac{z_{Q-1}+z_Q}{2}}^{z_{Q+1}} P_p(x)dx \end{cases} \tag{9}$$

B. K-Medoids Based PV Solar Power Scenario Fusion and Reduction

The optimal discrete quantiles of solar output can be obtained at hour intervals based on the approach introduced in Section II-A. However, for a n-hour scheduling problem, multi-period scenario generation of solar power need to be performed. By assuming that the scheduling time horizon is T and by denoting the number of optimal discrete quantiles at tth hour as Q_t, the total number of generated solar power scenarios can be determined as $N = \prod_{t=1}^{T} Q_t$. Since N increases exponentially with the increase of T, the curse of dimensionality would be incurred. To tackle this issue, the scheduling time T is divided into multiple sub-intervals, and clustering is performed to reduce scenarios for each sub-interval. By assuming that T is divided into M multiple sub-intervals and that each sub-interval m (m=1, 2,…, M) includes T_m hours, T is calculated as: $T = \sum_{m=1}^{M} T_m$. The number of scenarios of the T_m hours is $N_m = \prod_{t\in T_m} Q_t$, the probability of each sub-interval is $P_m = \prod_{i=t}^{i+T_m-1} P_m^q$, where P_m^q is the probability of a discrete quantile z_q in the sub-interval m.

After the time division process, scenario reduction is performed to reduce the number of the scenarios for sub-interval period T_m. By denoting d (u^i, u^j) as the distance between two scenarios u^i and u^j in the initial scenario set S, and as J_r the reduced scenario set which consists of K scenarios, the optimal scenario set J_r is then obtained by solving:

$$\min \sum_{\substack{u^i \in S \\ u^i \notin J_r}} p_i \min d(u^i, u^j) \tag{10}$$

where p_i is the probability of the scenario u^i. Eq. (10) represents the objective of the scenario reduction, i.e., to minimize the probability distance between the deprecated set and reserved scenario set. In this manner, finding J_r is similar to clustering, which classifies objects into different groups so that each group has similar properties. In this study, K-medoids [25] is employed to classify all scenarios into K categories.

The cluster center is iteratively updated in each category until one of the following conditions is satisfied: (a) the value of $\sum_{u^i \in J_n} p_i \min_{u^j \notin J_n} d(u^i, u^j)$ is smaller than a pre-specified threshold; or (b) the maximum iteration time is reached. Based on reduced scenarios set of each sub-interval, Cartesian product method is then used to merge the scenario set for all neighboring sub-intervals. After that, scenario fusion and reduction process are repeated until all time intervals are covered (Fig.1). Based on this, the reduced solar power scenarios can then be obtained.

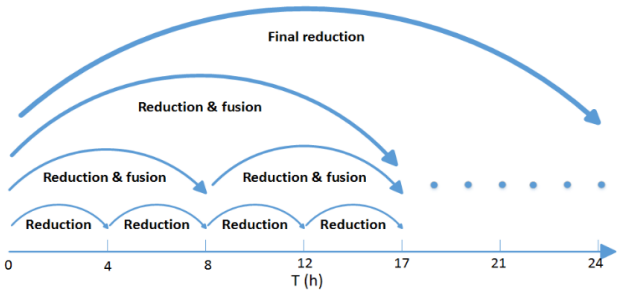

Fig. 1. Process of K-medoids based scenario fusion and reduction

III. Hierarchical Home Energy Management System

HERs considered in this study include: a RBESS, multiple controllable appliances, and a rooftop solar panel. The controllable appliances are further categorized into interruptible controllable appliances (ICAs) and non-interruptible controllable appliances (NICAs), respectively. ICAs refer to appliances whose operations can be interrupted temporally and resumed later, such as clothes dryer and washing machine; NICAs refer to appliances whose operations cannot be interrupted, such as roaster and coffee maker.

As shown in Fig. 2, the proposed HEMS is organised in a hierarchical structure that coordinates HER scheduling and controls the two day-ahead and actual operation stages. In the day ahead stage, operational requirements of the controllable appliances are specified by the user. Then, the HEMS performs day-ahead scheduling to determine to operation plans of the RBESS and controllable appliances, with the objective of minimizing the expected home electricity cost. The uncertainty of photovoltaic solar power is modelled by using the scenario analysis method presented in Section II. After day-ahead scheduling, schedules of controllable appliances are determined and the user is informed about the appliance schedules. When the actual operation stage arrives, based on the realization of solar radiation, the HEMS updates RBESS charging/discharging actions through a proposed SSRHO scheme, with the objective to minimize the actual home electricity cost.

A. Day-Ahead Stage: Stochastic HER Day-Ahead Scheduling Model

Based on the scenario analysis presented in Section 2, the day-ahead HER scheduling model is formulated as Eq. (11).

$$\min F_1 = \sum_{o \in O} \rho_o C_o^{grid} + C^{bess} \tag{11}$$

where C_o^{grid} is the electricity purchase cost from the grid under solar power scenario o; C^{bess} is RBESS operation cost. These two items are calculated as:

$$C_o^{grid} = \sum_{t=1}^{T} \left[pr_t \Delta t \cdot \max(L_{o,t}^{net}, 0) \right] \tag{12}$$

$$L_{o,t}^{net} = \sum_{a \in \Phi} s_{a,t} P_a^{ca,*} + L_t + P_t^{bess} - P_{o,t}^{pv} \tag{13}$$

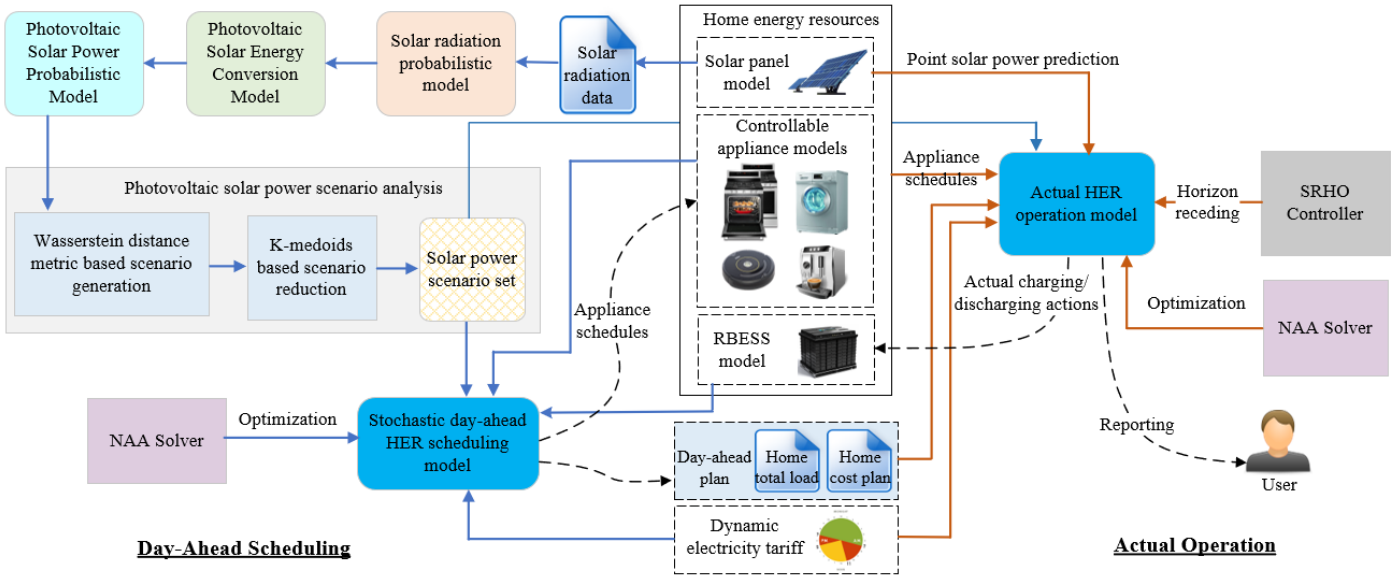

Fig. 2. Schematic of the proposed HEMS

$$P_a^{ca,*} = \begin{cases} P_a^{ca} & \text{if } s_{a,t} == 1 \\ P_a^{ca,base} & \text{if } s_{a,t} == 0 \end{cases} \tag{14}$$

$$C_{bess} = \sum_{t=1}^{T} \left(\gamma \cdot P_t^{bess} \cdot \Delta t + \gamma \cdot E_t^{bess} \cdot \eta^l \cdot \Delta t \right) \tag{15}$$

Decision variables of model (11) include the ON/OFF operations of controllable appliances ($s_{a,t}$) and charging/discharging power of the RBESS (P_t^{bess}). Model (11) is subjected to the following constraints:

(a) RBESS operational constraints.

$$\left| P_t^{bess} \right| \le P^{bess,rate} \quad \forall t = 1:T \tag{16}$$

$$SOC^{\min} \le SOC_t \le SOC^{\max} \quad \forall t = 1:T \tag{17}$$

$$SOC_t^{bess} = E_t^{bess} \big/ E^{bess,rate} \quad \forall t = 1:T \tag{18}$$

$$E_{t+1}^{bess} = \begin{cases} E_t^{bess} + \Delta t \eta^c P_t^{bess} - E_t^{bess} \eta^l \Delta t & P_t^{bess} > 0 \\ E_t^{bess} - |P_t^{bess}| \eta^d \Delta t - E_t^{bess} \eta^l \Delta t & P_t^{bess} \le 0 \end{cases} \quad \forall t = 1:T-1 \tag{19}$$

$$SOC_T \ge SOC^{desire} \tag{20}$$

Eqs. (16) and (17) represent the rated power and allowable SOC limit constraints; Eq. (20) ensures that, at the end of the day, the SOC of the RBESS does not fall below a pre-specified threshold (SOC^{desire}), so that it can continuously serve the house in the incoming day.

(b) Controllable appliance operation time constraint. Controllable appliances must operate within the time ranges specified by the user:

$$s_{a,t} = 0, \quad \forall a \in \Phi, t < t_a^{start}, t > t_a^{end} \tag{21}$$

(c) Operation cycle constraint of controllable appliances. When the task is finished, the appliance must be turned off:

$$\sum_{t=1}^{T} (s_{a,t} \cdot \Delta t) = d_a \quad \forall a \in \Phi \tag{22}$$

(d) NICA operation constraint. The operation of NISA cannot be interrupted until it finishes its work:

$$\sum_{t=t_{a''}^*}^{t_{a''}^* + d_{a''}/\Delta t} s_{a'',t} = 1 \quad \forall a'' \in \Phi^{NICA} \tag{23}$$

where $t_{a''}^*$ represents the time interval when the NISA a'' is activated in the first instance.

(e) ICA minimum online/offline time constraints. For ICA, the minimum online and offline time constraint is applied to protect their mechanical devices, shown as：

$$\begin{cases} \tau_{a',t}^{on} \ge \tau_{\min,i}^{on} & s_{a'}(t) == 0 \\ \tau_{a',t}^{off} \ge \tau_{\min,i}^{off} & s_{a'}(t) == 1 \end{cases} \quad \forall a' \in \Phi^{ICA}, \ t = 1:T \tag{24}$$

Decision variables of the day-ahead scheduling model (Eqs. (11)-(24)) include ON/OFF status of the controllable appliances ($s_{a,t}$) and charging/discharging power of the RBESS (P_t^{bess}) .

B. Semi-Scenario Based Rolling Horizon Optimization Scheme

As a useful control technique, RHO provides a way to control a process with real-time realization of stochastic variables. RHO provides continuous predictions to stochastic variables over a moving prediction horizon, and applies control actions to the process based on realization of the current time point. RHO has already been applied on many power system applications, such as [26-28]. A conventional RHO is generally characterized by following steps:

(a) *Prediction*. The stochastic variables and associated system model behaviours are predicted over a future horizon, called the predictive window;

(b) *objective function definition*. The closed-loop performance of the system model over the prediction window is specified;

(c) *objective function optimization*. The objective function is optimized as a function of the set of future control signals to be applied to the system model during the predictive window; and

(d) *receding horizon strategy*. Only the control signal of the first one or first *n* time interval (called the control window) is applied to the real system. In the subsequent time step, the predictive window moves forward with one or *n* time intervals, and entire algorithm is repeated.

In conventional RHO, point prediction is performed on the stochastic variables over the prediction window. To ensure the real-time prediction accuracy, the prediction window size cannot be too large. A variation of RHO is proposed in [29, 34, 25], which uses scenario analytics to replace point prediction in conventional RHO, so as to sufficiently consider uncertainties of the stochastic variables. However, for very short-term forecasting (e.g. several minutes or hours ahead), point prediction can normally achieve high accuracy while scenario analytics would bring unnecessary extra computational cost. Based on this consideration, a new RHO variant is proposed and denoted as Semi-Scenario based Rolling Horizon Optimization. Different from (a) the conventional RHO fully based on a point prediction and (b) the fully stochastic RHO [29, 34, 35] fully based on scenarios, the proposed SSRHO simultaneously integrates both point prediction and scenario analytics by consisting of a *point prediction window* and a *scenario window*.

The point prediction window represents the horizon where the very short-term point prediction is applicable; the scenario window represents the horizon where the accurate very short-term prediction is difficult to be achieved. The scenario set of the stochastic variables is generated over the scenario window. In each iteration, both the point prediction window and scenario window are considered, and the objective function can be defined on both point prediction window and scenario window. Comparison of the workflow of both conventional RHO and SSRHO are illustrated in Fig. 3.

C. SSRHO Based HER Actual Operation Model

In each SSRHO round, the very short-term point forecasting of PV solar power is performed over the prediction window, and the solar power scenario set is generated over the scenario window, using the methodology described in Section II. An objective function is defined to minimize the home electricity cost over both the prediction window and scenario window:

$$\min F_2 = C^{bess,srho} + C^{grid,pd} + C^{grid,sn} \tag{25}$$

$$C^{bess,srho} = \sum_{t=t^{st}}^{t^{st}+T^{pd}+T^{sn}} \left(\gamma \cdot P_t^{bess,srho} \cdot \Delta t + \gamma \cdot E_t^{bess,srho} \cdot \eta^l \cdot \Delta t \right) \tag{26}$$

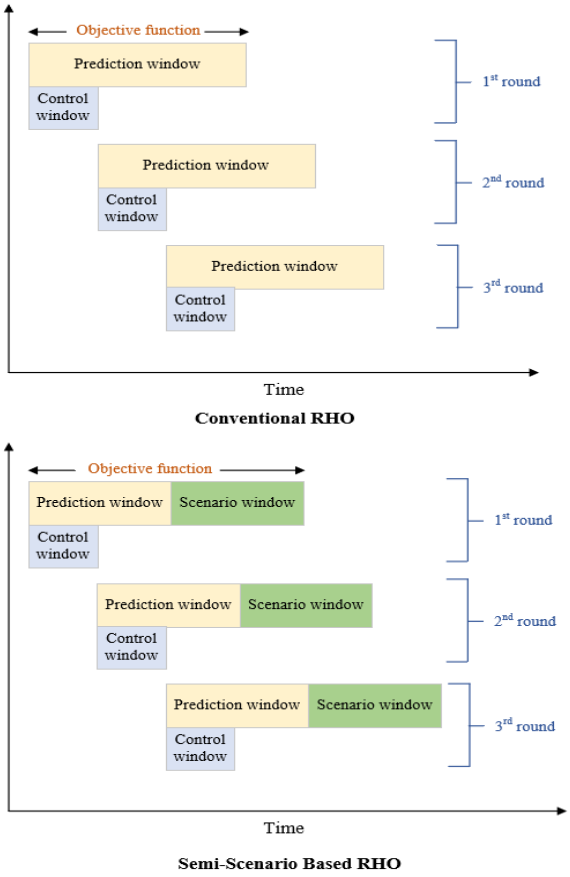

Fig. 3. Illustrations of conventional RHO and SSRHO

$$C^{grid,pd} = \sum_{t=t^{st}}^{t^{st}+T^{pd}} \left[pr_t \Delta t \cdot \max(L_t^{net,pd}, 0) \right] \tag{27}$$

$$L_t^{net,pd} = L_t^{srho} + P_t^{bess,shro} - P_t^{pv,pd} \tag{28}$$

$$C^{grid,sn} = \sum_{o \in O} \rho_o \left\{ \sum_{t=t^{st}+T^{pd}}^{t^{st}+T^{pd}+T^{sn}} \left[pr_t \Delta t \cdot \max(L_{o',t}^{net,sn}, 0) \right] \right\} \tag{29}$$

$$L_{o,t}^{net,sn} = L_t^{srho} + P_t^{bess,shro} - P_{o,t}^{pv,sn} \tag{30}$$

where $C^{bess,srho}$ is the RBESS operation cost over the SSRHO horizon; $C^{grid,pd}$ and $C_t^{bess,act}$ represent the actual home electricity cost and RBESS operation cost at time t; $C^{grid,pd}$ and $C^{grid,sn}$ are expected electricity purchase costs over the prediction window and scenario window, respectively; t^{st} represents the starting time interval of the current SSRHO round; $L_t^{net,pd}$ represents the home net-load at time t of the prediction window; $L_{o,t}^{net,sn}$ represents the home net-load at time t of the scenario window under scenario o. The decision variable of the model (25) is the charging/discharging power of the RBESS at the actual operation stage ($P_t^{bess,srho}$) and is sought by applying the RBESS operational constraints (16)-(20).

IV. Solving Approach

The day-ahead scheduling model (11) is a constrained, mix-integer, nonlinear optimization problem over a finite horizon; the actual operation model (25) is a constrained, continuous optimization problem. Solving of model (11) is computational difficult due to its mix-integer, nonlinear and high dimensional natures. We employ a metaheuristic algorithm previously proposed by the authors, i.e. Natural Aggregation Algorithm (NAA) [30], to solve the model (11), and use the Matlab Optimization Toolbox to solve model (23). NAA has shown strong global exploration capabilities on several power system optimization problems, e.g. [31-33].

A. Encoding Scheme of the HER Day-Ahead Scheduling Model in NAA

By applying NAA to solve the day-ahead scheduling model (11), each individual is encoded as a vector with $\left|\Phi^{NICA}\right| + \left|\Phi^{ICA}\right| \cdot T + T$ dimensions, respectively, representing a potential day-ahead HER scheduling solution. The first $\left|\Phi^{NICA}\right|$ dimensions represent the starting operation time of each NICA (integer variables). When the starting operation time of the NICA is determined, its end operation time is determined based on the NICA's operation cycle duration. The next $\left|\Phi^{ICA}\right| \cdot T$ dimensions represent states of ICAs over the T time intervals (binary variables), while the last T dimensions represent the charging/discharging power of the RBESS.

B. Overall Solving Workflow

The overall workflow of the HEMS is illustrated in Fig. 4. In the day-ahead stage, parameter values of Beta distribution are learned from the historical solar radiation data. The solar power probabilistic distribution is then obtained from the photovoltaic solar power conversion model. Based on this, the solar power output scenarios are generated. The solar power scenarios are inputted into the day-ahead HER scheduling model, together with the controllable appliance models, TOU tariff information, forecasted home load, and the RBESS model. NAA solver is then applied to solve the day-ahead HER scheduling model.

In the actual operation stage, the appliance operation schedules, which are generated from the day-ahead scheduling, are inputted into the actual operation model, together with the actual solar power output and actual home load. The Matlab Optimization Toolbox is applied to solve the actual operation model, and the SSRHO process is applied to recede both the prediction and scenario windows.

V. Simulation Study

A. Simulation Setup

A smart home environment in a spring day is simulated. The must-run home load, i.e., the house's power consumption excluding controllable appliances and RBESS, is modified from a residential house data of the Australian "Smart Grid, smart City" dataset. An Australian 1-year solar radiation dataset is used for the residential PV solar simulation. We consider nine controllable appliances: a dish washer, a clothes dryer, a rice cooker, a washing machine, a pool pump, a robot

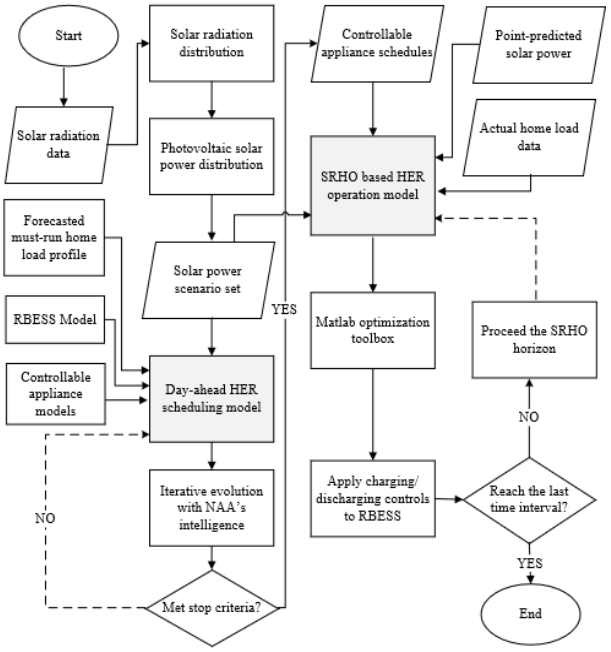

Fig. 4. Workflow of the hierarchical HEMS

vacuum cleaner, a coffee machine, and an oven, with configurations summarized in table I. The pool pump, dish washer, clothes dryer, washing machine, and robot vacuum cleaner are Interruptible, while other appliances are treated as non-interruptible. Configurations of the RBESS is given in table II. The time-of-use tariff in this simulation is shown in table III. Control parameters of NAA and SSRHO are set as table IV.

B. Evaluation of the Solar Power Scenario Analytics Approach

The efficiency of the proposed approach is investigated in the following by comparing its performance in terms of scenario approximation accuracy obtained against the results obtained using other conventional scenario generation algorithms that include the Monte-Carlo sampling, the ARMA, and the Latin Hypercube Sampling (LHS). Each algorithm is applied to generate a scenario set W containing 1,000 solar power scenarios. 10^6 scenarios are then sampled as the base scenario set according to the original continuous probability distribution. The distance metric D of scenario set W, $D = \sum_{u^i \in Y} p_i \min_{u^j \in W} d(u^i, u^j)$, is used to determine the efficiency of the algorithms. A small value of D indicates a large approximation accuracy. The comparison results are shown in Fig.5. It is clear that the developed approach shows a better approximating accuracy improvement when compared to the other algorithms. ARMA does not consider the random quantities of each time interval, and thus has the worst approximation accuracy.

The computational efficiency of the approach is then compared against the one possessed by the conventional Fast Forward Selection (FFS) method. The results are reported in table V. For FFS, firstly 3,000 random scenarios are generated and the FFS is then applied to reduce the scenario number by reserving representative scenarios. The results show that the total execution time of K-medoids clustering (4.17s) is well below the one obtained with the FFS (526s). These comparisons highlight how the proposed approach can achieve satisfa-ctory scenario approximation accuracy with a fast computing speed. This is mainly attributed to the parallel architecture of the method in which scenarios of each sub-interval are not related. This advantage is particularly significant for home energy management, where the HEMS is often implemented and deployed in devices with limited computing power.

C. Day-Ahead Scheduling Results

Using the scenario analysis presented in Section II, seven PV power output scenarios are generated, as shown in Fig. 6. The day-ahead home energy resource scheduling model is then solved, with the results reported in Figs. 7 and 8. Fig. 7 shows the charge/discharge power of the RBESS and the corresponding SOC profile, respectively. Scheduling results of the controllable appliances are shown in Fig. 8.

TABLE I
CONFIGURATIONS OF THE CONTROLLABLE APPLIANCES

Name	Operation duration	Operation time range	P_a^{ca}	$P_a^{ca,base}$
Pool pump	3hours	[10am, 5pm]	1.5 kW	0.1kW
Dish washer	1.5hours	[8:30pm, 7am]	2.4 kW	0.2kW
Washing machine	1.5hours	[11pm, 7am]	0.9 kW	0.1kW
Rice cooker	0.75hours	[11:30am, 2pm; 5pm, 7pm]	0.6 kW	0kW
Clothes dryer	1.75hours	[9am, 6:30pm]	2.5 kW	0.2kW
Vacuum cleaner	2hours	[9am, 6pm]	0.7kW	0.1kW
Coffee machine	0.25 hours	[9am, 2pm]	0.8kW	0kW
Oven	1 hour	[11am, 4pm]	2.1 kW	0kW

TABLE II
SETTINGS OF THE RBESS

Power Capacity	Energy Capacity	SOC^{desire}
3kW	12kWh	30%
SOC Lower Limit	SOC Upper Limit	γ
10%	90%	0.1
η^c	η^l	Initial SOC
90%	90%	30%

TABLE III
TIME-OF-USE ELECTRICITY TARIFF

Time-of-Use Tariff	Rate ($/kWh)
Peak: 2-8 PM	0.3564
Shoulder: 7AM-2PM, 8-10PM	0.1408
Off-Peak: 10PM-7AM	0.0814

TABLE IV
SETTINGS OF NAA AND SSRHO

NAA Setting			
	Parameter Name	Meaning	Value
Overall Control	N^{pop}	Population size	200
	$G^{\max}$	Maximum generation time	800
Sub-Population Control	N^S	Number of shelters	10
	Cp^S	Shelter capacity	20
Located Search Control	δ	Scaling factor	1
	Cr_{local}	Located crossover factor	0.6
Generalized Search Control	α	Movement Amplification	1.5
	Cr_{global}	Generalized crossover factor	0.3

SSRHO Setting	
Parameter Name	Value
Prediction window	4 hours
Scenario window	20 hours
Time Interval Duration	15 minutes

TABLE V
COMPUTATIONAL EFFICIENCY COMPARISON OF THE DEVELOPED APPROACH AND FFS

Reduced scenarios	Our method		FFS time/s
	Iterations	Time/s	
1000	28	0.56	79
500	35	1.17	151
200	54	2.39	324
5	67	4.17	526

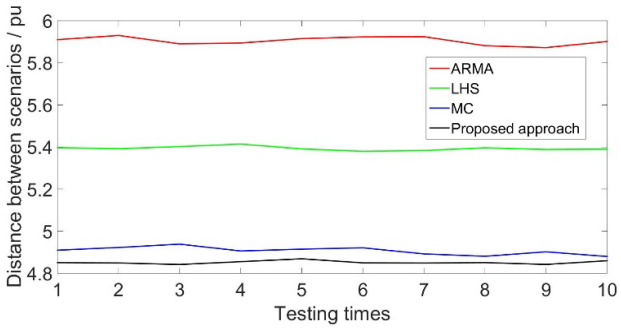

Fig. 5. Representative tests for scenario sets under four methods

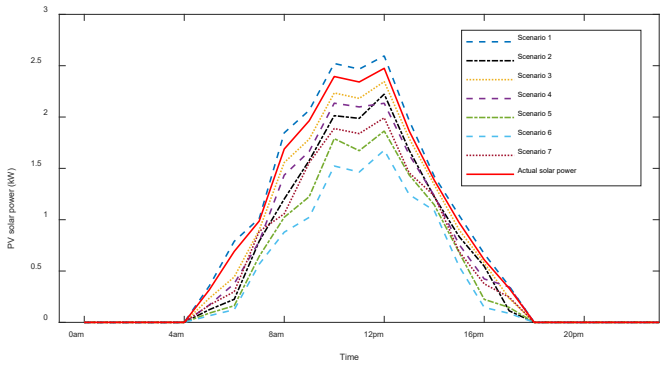

Fig. 6. Workflow of the hierarchical HEMS

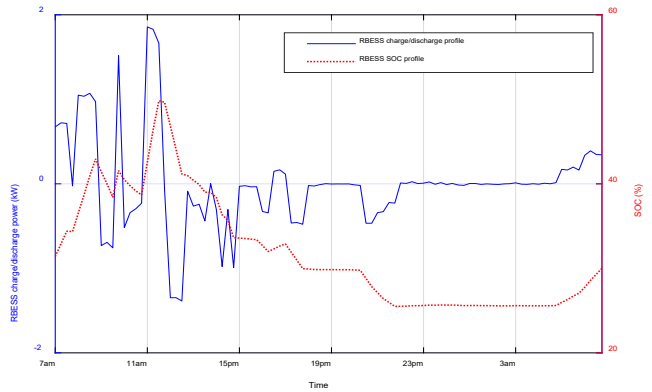

Fig. 7. Day-ahead RBSS operation plan

The result shows that the appliances are well scheduled to operate within the allowable time ranges. The large power consumers, i.e. pool pump and oven, are scheduled to operate at noon, when the solar power is sufficient. As another large power consumer, while the allowable operation time range is [8:30pm, 7am], the dish washer is scheduled to run around

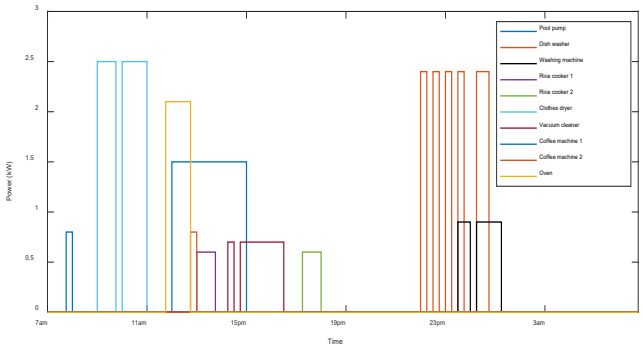

Fig. 8. Operation schedules of controllable appliances

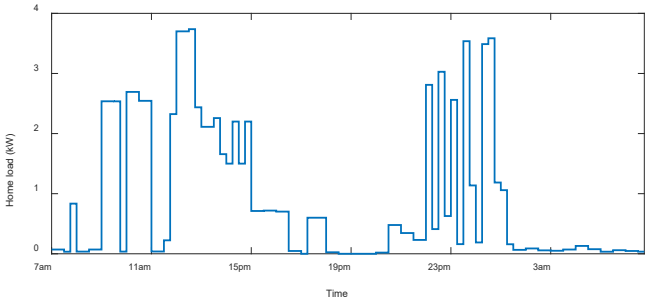

Fig. 9. Total home load profile

23pm, when the TOU price is lowest. Other appliances are also well scheduled to satisfy the user's lifestyle requirements. Together with the controllable appliances, the RBESS is scheduled to operate as depicted in Fig. 7. However, its operation will be updated in the actual operation stage by the SSRHO.

With determination of the appliances' schedules, the total home load profile is determined, as shown in Fig. 9. In the actual operation stage, the SRHO is applied to update the RBESS operation, with the results reported as below.

D. Actual Operation Results

By applying the SSRHO and proceed the optimization horizon, the RBESS is controlled to accommodate the realization of the solar power. After 24-hour iterative operation of the SSRHO, the charging/discharging profile and corresponding SOC profile of the RBESS are shown in Fig. 10. Fig. 10 shows the final charging/discharging profile of the RBESS together with the profiles of the total home load and actual solar power.

The actual RBESS operation results show some similar trend with the day-ahead plan in Fig. 7. In the morning and noon time when there is sufficient solar power and the RBESS is charged. In the afternoon, when the solar power is less and the home load is relatively high, the RBESS discharges to serve the home consumption. Comparing Figs. 7 and 10, it can be seen that with the continuous realization of solar power and proceeding of the SSRHO, the RBESS schedule is continuously updated and deviates from the day-ahead plan to some extent. For example, by taking into account different possible solar power scenarios, in the day-ahead plan the RBESS is scheduled to not charge or discharge at night (around 10pm to 2am). In the actual operation, since the RBESS has been sufficiently charged in the daytime, it is scheduled to discharge to

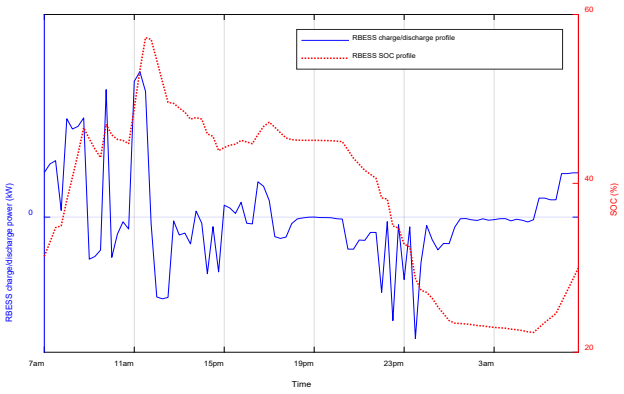

Fig. 10. Actual RBESS operation results

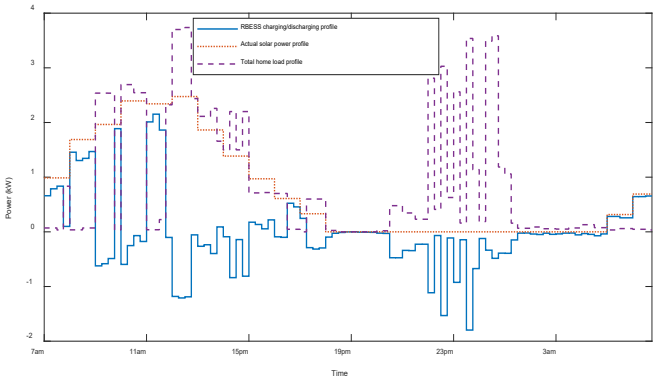

Fig. 11. Actual operation results of the home microgrid

TABLE VI
COMPARISON STUDY OF CASES WITH AND WITHOUT SRHO

	Without HEMS	Without SSRHO	With conventional RHO	With SSRHO
Total cost	1.61$	0.95$	0.81$	0.66$
Energy purchase cost	1.61$	0.71$	0.44$	0.34$
RBESS operation cost	0$	0.24$	0.37$	0.32$
Total energy purchased from grid	8.88kWh	6.29kWh	5.23$	4.16kWh

serve the washing machine and dish washer (and other must-run home loads) during this period. The final actual operation results of the day are visualized in Fig. 11.

To further illustrate the effectiveness of the proposed HEMS, we design a comparison study to compare the proposed system with three benchmark cases. In the first benchmark case, there is no HEMS. This implies the scenario where no RBESS is installed and the solar power is directly used to serve the home load. In this case, also the controllable appliances are not scheduled and their operations are set to start at the beginning of the allowable time range. In the second base case, both RBESS and controllable appliances are scheduled, but no RHO is applied to update the RBESS operation. This implies that the RBESS strictly follows the day-ahead plan (Fig. 7) in the actual operation stage. In the third benchmark case, we apply the conventional RHO technique [28]. In this case, we add Gaussian distributed noise data with expectation of 0 and deviation of 0.5 into the actual solar power output profile to simulate the forecasted solar power data produced by point prediction. In the third benchmark case, there is therefore no scenario window, but only a point prediction window of four hours. The main home operation results under the three cases are summarised in table VI. The results clearly show that without HEMS, the one-day electricity cost of the home is relatively high, i.e. 1.61$. By using HEMS to perform stochastic day-ahead scheduling, the home electricity cost is reduced to 0.95$. With conventional RHO, proper update for the RBESS can be performed, and the total home electricity cost is thus reduced to 0.81$. Since the relatively accurate point prediction only covers four hours, it is difficult for the conventional RHO to produce an optimal solution over the whole operation period. By using the proposed SSRHO to update the RBESS operation in the actual operation stage, the energy purchase cost is further reduced to 0.34$, with a slight increase of RBESS operation costs (0.32$).

VI. CONCLUSIONS

This paper proposes a hierarchical energy management system for smart homes. The system firstly performs scenario analysis for the residential PV solar power by using the Wasserstein distance metric-based scenario generation and K-medoids based scenario fusion and reduction techniques. Based on the generated solar power scenario set, the system performs two-stage energy management. In the day-ahead stage, it establishes a stochastic day-ahead scheduling model to determine the appliance schedules. In the actual operation stage, it uses a new stochastic rolling horizon optimization mechanism to update the RBESS operation. The simulation results show that this hierarchical energy management system and effectively schedules both the controllable appliances and the RBESS to significantly reduce the home electricity cost, better utilize the residential renewable energy, and thus improve energy efficiency of the demand side.

ACKNOWLEDGEMENTS

The authors would like to acknowledge Mrs. Xiaodan Wang from The NextGen Strata Pty Ltd, Australia, for her assistance on simulation scenario setup.

REFERENCES

[1] The Home Microgrid: Not Later. Now. [Online]. Available at: https://microgridknowledge.com/home-microgrid-later-now/
[2] Z. Zhao, W. Lee, Y. Shin, and K. Song, "An optimal power scheduling method for demand response in home energy management system," *IEEE Transactions on Smart Grid*, vol. 4, no. 3, pp. 1391-1400, 2013.
[3] M.A. Pedrasa, T. Spooner, and I. MacGill, "Coordinated scheduling of residential distributed energy resources to optimize smart home energy services," *IEEE Transactions on Smart Grid*, vol. 1, no. 2, 2010.
[4] M. Rasteger, M. Fotuhi-Firuzabad, and F. Aminifar, "Load commitment in a smart home," *Applied Energy*, vol. 96, pp. 45-54, 2012.
[5] Y. Ozturk, D. Senthilkumar, S. Kumar, and G. Lee, "An intelligent home energy management system to improve demand response," *IEEE Transactions on Smart Grid*, vol. 4, no. 2, pp. 694-701, 2013.
[6] Y. Iwafune, T. Ikegami, etc., "Cooperative home energy management using batteries for a photovoltaic system considering the diversity of households," *Energy Conversion and Management*, vol. 96, 2015.
[7] D. Nguyen and L.B. Le, "Joint optimization of electric vehicle and home energy scheduling considering user comfort preference," *IEEE Transactions on Smart Grid*, vol. 5, no. 1, pp. 188-199, Jan. 2014.
[8] A. Mohsenian-Rad and A. Leon-Garcia, "Optimal residential load control with price prediction in real-time electricity pricing environments," *IEEE Transactions on Smart Grid*, vol. 1, no. 2, pp. 120-133, 2010.
[9] W. Li, K. Thirugnanam, W. Tushar, C. Yuen, and K. Chew, "Improving the operation of solar water heating systems in green buildings via opti-

mized control strategies," *IEEE Transactions on Industrial Informatics*, vol. 14, no. 4, pp. 1646-1655, 2018.
[10] F. Luo, G. Ranzi, W. Kong, Z.Y. Dong, and F. Wang, "Coordinated residential energy resource scheduling with vehicle-to-home and high photovoltaic penetrations," *IET Renewable Power Generation*, in press.
[11] F. Luo, G. Ranzi, X. Wang, and Z.Y. Dong, "Service recommendation in smart grid: vision, technologies, and applications," in *Proc. 9th International Conference on Service Science*, 2016.
[12] F. Luo, G. Ranzi, W. Kong, etc., "Non-intrusive energy saving appliance recommender system for smart grid residential users," *IET Generation, Transmission, and Distribution*, 2017.
[13] F. Luo, G. Ranzi, X. Wang, and Z.Y. Dong, "Social information filtering based electricity retail plan recommender system for smart grid end users," *IEEE Transactions on Smart Grid*, 2017.
[14] S. Squartini, M. Boaro, F. Angelis, etc., "Optimization algorithms for home energy resource scheduling in presence of data uncertainty," in *Proc. 4th International Conference on Intelligent Control and Information Processing*, Beijing, China, Jun 9-11, 2013.
[15] A.J. Roscoe and G. Ault, "Supporting high penetrations of renewable generation via implementation of real-time electricity pricing and demand response," *IET Renewable Power Generation*, vol. 4, no. 4, pp. 369-382, 2010.
[16] X. Chen, T. Wei, and S, Hu, "Uncertainty-aware household appliance scheduling considering dynamic electricity pricing in smart home," *IEEE Transactions on Smart Grid,* vol. 4, no. 2, pp. 932-941, 2013.
[17] R. Godina, E. Rodrigues, E. Pouresmaeil, J. Matias, and J. Catalao, "Model predictive control home energy management and optimization strategy with demand response," *Applied Sciences*, 2018.
[18] R. Godina, E. Rodrigues, E. Pouresmaeil, and J. Catalao, "Optimal residential model predictive control energy management performance with PV microgeneration," *Computers and Operations Research*, vol. 96, pp. 142-155, 2018.
[19] E. Rodrigues, R. Godina, E. Pouresmaeil, J. Ferreira, and J. Catalao, "Domestic appliances energy optimization with model predictive control," *Energy Conversion and Management*, vol. 142, pp. 402-413, 2017.
[20] D. Oliveria, E. Rodrigues, R. Godina, T. Mendes, J. Catalao, and E. Pouresmaeil, "Enhancing home appliances energy optimization with solar power integration," in *Proc. IEEE International Conference on Computer as a Tool*, 2015.
[21] X. Fu, Q. Guo, H. Sun, Z. Pan, and W. Xiong, "Typical scenario set generation algorithm for an integrated energy system based on the Wasserstein distance metric," *Energy*, Vol. 135, pp. 153–170, 2017.
[22] J. Shi, W. J. Lee, Y. Liu, Y. Yang, and P. Wang, " Forecasting power output of photovoltaic systems based on weather classification and support vector machines," *IEEE Trans. Ind. Appl.,* May. 2012..
[23] Q. Wang, W. L. Dong, L. Yang, "A wind power/ photovoltaic typical scenario set generation algorithm based on Wasserstein distance metric and revised K-medoids cluster" *Proceedings of the CSEE,* vol. 35, pp. 2654–2661, Jun, 2015
[24] S.W. Wallace, M. Kaut, "Evaluation of scenario-generation methods for stochastic programming" *Pacific journal of Optimization*, 2007.
[25] T.S. Madhulatha, "Comparison between K-Means and K-Medoids Clustering Algorithms," *Advances in Computing and Information Technology*, vol.198, pp. 472-481, 2011.
[26] J. Silvente, G. Kopanos, E.N. Pistikopoulos, etc., "A rolling horizon optimization framework for the simultaneous energy supply and demand planning in microgrids," *Applied Energy*, vol. 155, pp. 485-501, 2015.
[27] F. Luo, G. Ranzi, and Z.Y. Dong, "Rolling horizon optimization for real-time operation of thermostatically controlled load aggregator," *Journal of Modern Power Systems and Clean Energy*, vol. 5, no. 6, pp. 947-958, 2017.
[28] R. Palma-Behnke, C. Benavides, F. Lanas, etc., "A microgrid energy management system based on rolling horizon strategy," *IEEE Transactions on Smart Grid*, vol. 4, no. 2, pp. 996-1006, 2013.
[29] L. Meng and X. Zhou, "Robust single-track train dispatching model under a dynamic and stochastic environment: a scenario-based rolling horizon solution approach," *Transportation Research Part B: Methodological*, vol. 45, no. 7, pp. 1080-1102, 2011.
[30] F. Luo, J. Zhao, and Z.Y. Dong, "A new metaheuristic algorithm for real-parameter optimization: natural aggregation algorithm," in *Proc. IEEE Congress on Evolutionary Computation*, 2016.
[31] Y. Zheng, K. Meng, F. Luo, J. Qiu, and J. Zhao, "Optimal integration of mobile/stationary battery energy storage systems in distribution systems with renewables," *IET Renewable Power Generation*, 2018.
[32] G. Liang, S. Weller, F. Luo, J. Zhao, and Z.Y. Dong, "Generalized FDIA-based cyber topology attack with application to the Australian electricity market trading mechanism," *IEEE Transactions on Smart Grid*, vol. PP, no. 99, 2017.
[33] G. Liang, S. Weller, J. Zhao, F. Luo, and Z.Y. Dong, "A framework for cyber-topology attacks: line-switching and new attack scenarios," *IEEE Transactions on Smart Grid*, vol. PP, no. 99, 2017.
[34] G. Ripaccioli, D. Bernardini, S.D. Cairano, A. Bemporad, and I.V. Kolmanovsky, "A stochastic model predictive control approach for series hybrid electric vehicle power management," in *Proc. 2010 American Control Conference*, 2010.
[35] J.A. Primbs and C.H. Sung, "Stochastic receding horizon control of constrained linear systems with state and control multiplicative noise," *IEEE Transactions on Automatic Control*, vol. 54, no. 2, pp. 221-230, 2009.

Fengji Luo (SM'09, M'13) received his bachelor and master degrees in Software Engineering from Chongqing University, China in 2006 and 2009. He received his Ph.D degree in Electrical Engineering from The University of Newcastle, Australia, 2014. Currently, he is a Lecturer and Academic Fellow in the School of Civil Engineering, The University of Sydney, Australia. His research interests include energy demand side management, smart grid, smart building, and energy informatics. He has published over 100 papers on peer referred journals and conferences. He receives the Pro-Vice Chancellor's Research and Innovation Excellence Award of The University of Newcastle in 2015, the Australia-Japan Emerging Research Leader Award in 2016, and the UUKI Rutherford Fellowship in 2018.

Gianluca Ranzi (M'16) was awarded a degree in Management and Production Engineering at the Politecnico di Milano, Italy, a BE (Hons 1) at the University of Wollongong, Australia, a degree in Civil Engineering at the Universita' Politecnica delle Marche, Italy, and a PhD at the University of New South Wales (Australia). He is currently an Australian Research Council Future Fellow, professor and Director of the Centre for Advanced Structural Engineering at the University of Sydney, Australia. His research interests include smart buildings, structural engineering, building-to-grid technology, and demand side management.

Shu Wang (SM'15) received the B.S. degree in Electrical Engineering from the University of Newcastle, Australian in 2015. He is currently working toward his Ph.D. degree in the School of Electrical Engineering and Telecommunications, The University of New South Wales, Sydney, Australia. His research interests include active distribution network, renewable energy, stochastic programming, and demand side management.

Zhao Yang Dong (F'16) obtained Ph.D. from the University of Sydney, Australia in 1999. He is now with the University of NSW (UNSW), Sydney, Australia. He is Director of UNSW Digital Grid Futures Institute, and Director of ARC Research Hub for Integrated Energy Storage Solutions. His immediate role is Professor and Head of the School of Electrical and Information Engineering, The University of Sydney. He was Ausgrid Chair and Director of the Ausgrid Centre for Intelligent Electricity Networks (CIEN) providing R&D support for the $600M Smart Grid, Smart City national demonstration project. He also worked as manager for (transmission) system planning at Transend Networks (now TASNetworks), Australia. His research interest includes smart grid, power system planning, power system security, load modeling, renewable energy systems, and electricity market. He has been serving/served as editor for several journals including served as an editor for IEEE Transactions on Smart Grid, IEEE Transactions on Sustainable Energy, IEEE PES Transaction Letters and IET Renewable Power Generation. He is an international Advisor for the journal of Automation of Electric Power Systems. He is Fellow of IEEE.